

A Framework for the Analysis of Second Order Projection Methods*

Zheming Zheng[†]

Bernd Simeon[‡]

Linda Petzold[§]

March 26, 2009

*This work was supported by the National Science Foundation under NSF awards NSF/ITR CCF-0428912

[†]Department of Mechanical Engineering, University of California Santa Barbara, Santa Barbara, CA 93106, USA.
Email: zhengzhm@engineering.ucsb.edu

[‡]Zentrum Mathematik, Technische Universität München, Boltzmannstr. 3, D-85748 Garching bei München,
Email: simeon@ma.tum.de

[§]Department of Mechanical Engineering, University of California Santa Barbara, Santa Barbara, CA 93106, USA.
Email: petzold@engineering.ucsb.edu

Abstract

In this paper we present a common framework for projection methods for the solution of incompressible Navier-Stokes systems. We address through both analysis and numerical experiments how the pressure update effects the temporal order and stability, and explain some observations that have been reported in the literature. Based on this framework, we propose an efficient procedure for obtaining second-order accuracy in time for the pressure, which works with a variety of projection methods.

Keywords: Projection methods; Incompressible Navier-Stokes equations; Stability analysis; Order analysis

1 Introduction

Projection methods were first proposed by Chorin [8] and Temam [23] for solving incompressible Navier-Stokes equations

$$\frac{\partial \mathbf{u}}{\partial t} + \nabla P = -(\mathbf{u} \cdot \nabla) \mathbf{u} + \frac{1}{Re} \nabla^2 \mathbf{u}, \quad (1a)$$

$$\nabla \cdot \mathbf{u} = 0, \quad (1b)$$

with boundary conditions

$$\mathbf{u}|_{\Gamma} = \mathbf{u}_b,$$

where \mathbf{u} is the velocity, P is the pressure and Re is the Reynolds number. To solve this problem, projection methods use a fractional step approach, in which an intermediate velocity is obtained by solving the momentum equation (1a) without regard to the incompressibility constraint (1b), and then a projection of the intermediate velocity onto the divergence-free space is performed to obtain the corrected velocity that satisfies the incompressibility constraint. The difficulty in solving Eq. (1) is that the pressure is coupled in the momentum equation, while the pressure itself does not evolve according to a differential equation. Rather, its value is determined by enforcing the incompressibility constraint. It has been observed that while the velocity can be reliably computed to second order accuracy in time, the pressure is typically only first-order accurate in time [9].

Since the projection methods were first proposed, they have attracted a great deal of research interest [4, 5, 19, 21, 6, 10, 7]. Over the past decades, numerous fractional-step, operator-splitting projection methods and their analysis have emerged. An overview of projection methods can be found in [7, 14]. An intermediate velocity \mathbf{u}^* is obtained by solving the momentum equation without regard to the incompressibility constraint, using an approximate value q of the pressure. The momentum equation is usually solved by implicit methods, such as the trapezoidal (Crank-Nicolson) method [4, 5, 7], the backward differentiation formula (BDF) method [14] and the alternating

direction implicit (ADI) method [21]. A projection is then performed on \mathbf{u}^* as follows

$$\mathbf{u}_{n+1} = \mathbf{u}^* - \Delta t \nabla \phi_{n+1}, \quad (2)$$

$$\nabla \cdot \mathbf{u}_{n+1} = 0. \quad (3)$$

Then the pressure is updated as

$$P_{n+\frac{1}{2}} = q + \phi_{n+1}. \quad (4)$$

q usually is chosen to be the pressure at the previous time step, $P_{n-\frac{1}{2}}$, in an incremental scheme. q can also be set to 0, where the method is referred to as the pressure-free method [19]. An improved pressure-update formula, also known as the rotational pressure-correction formula, is given in [31, 7, 28]:

$$P_{n+\frac{1}{2}} = q + \phi_{n+1} - \frac{\Delta t}{2Re} \nabla^2 \phi_{n+1}. \quad (5)$$

Besides the above projection methods, there are also many other projection-type methods. E and Liu [10] proposed the gauge method. By using an extrapolation in time, all variables can be computed to second order accuracy. Liu *et al.* [22] proposed a continuous projection method. Based on a local truncation error (LTE) analysis, they obtain a sufficient condition for the continuous projection methods to be temporally second-order accurate for both the velocity and the pressure. Dukowicz and Dvinsky [18] used an approximate factorization method to derive a projection method which is second order for the velocity and first order for the pressure. One can also directly take the divergence of Eq. (1a) and derive the so-called “pressure-Poisson” equation for the pressure [15, 12]. However this requires a boundary condition for the pressure which usually is difficult to obtain. One advantage of the projection methods is that they avoid the computation of a pressure boundary condition.

Brown *et al.* [7] surveyed some of the projection methods and speculated on the effects of boundary conditions and different pressure-update formulas on the order of accuracy. Because per-

forming the projection exactly on a cell-centered grid can cause numerical difficulties, approximate projection methods [2, 1] are often used instead. In these methods, the incompressibility constraint is only approximately satisfied. However, the approximate projection methods are highly sensitive to the grid structure and the method used and may be susceptible to instabilities [16]. A series of numerical issues related to the analysis and implementation of projection methods are summarized in [14].

In this paper we introduce a common framework for second order projection methods and show by analysis how the form of the projection update and a parameter which appears in the literature in the pressure update determine the order and stability properties of the method. We propose a sufficient condition for the pressure to be temporally second-order accurate, which is easy to implement and works with a variety of projection methods. The analysis successfully explains some observations that have been reported in the literature and the analysis results are verified by numerical experiments.

This paper is organized as follows. Two types of projection are introduced in Section 2. In Section 3 a common framework for projection methods is presented and an analysis of order and stability is performed for the second order projection methods. Some issues related to a class of projection methods in the literature, stability properties of a new projection method and boundary conditions we used are also discussed in this section. Numerical results are presented in Section 4, and conclusions are given in Section 5.

2 DAE Systems and Projections

In this section we introduce the differential-algebraic equation (DAE) methodology and notation that will be used in the analysis. Following the method of lines approach, the incompressible Navier-Stokes equations can be formulated as a DAE system by semi-discretization in space. The spatial discretization and associated boundary conditions will be discussed in the following. In this paper we focus on the temporal analysis of the system. The order in this paper means the temporal order,

if not explicitly noted. Since the convection term is usually computed explicitly, for simplicity, we will neglect the convection term and consider the Stokes equation

$$\frac{d\mathbf{u}}{dt} = A\mathbf{u} - GP, \quad (6a)$$

$$0 = D\mathbf{u}, \quad (6b)$$

with boundary conditions

$$\mathbf{u}|_{\Gamma} = \mathbf{u}_b,$$

where A denotes the discretized Laplacian ($\frac{1}{Re}\nabla^2$) operator matrix, and G and D denote the discretized gradient (∇) and divergence ($\nabla\cdot$) operators respectively. Boundary conditions are included in the matrices A , G and D , as described below.

Example for discretized boundary conditions

Consider a $nx \times ny$ staggered grid (e.g., 3×3 staggered grid shown in Figure 1), the DAE system (6) can be written as

$$\frac{du_{i,j}}{dt} = \frac{1}{Re} \left(\frac{u_{i+1,j} + u_{i-1,j} - 2u_{i,j}}{\Delta x^2} + \frac{u_{i,j+1} + u_{i,j-1} - 2u_{i,j}}{\Delta y^2} \right) - \frac{P_{i,j} - P_{i-1,j}}{\Delta x}, \quad (7a)$$

$$\frac{dv_{i,j}}{dt} = \frac{1}{Re} \left(\frac{v_{i+1,j} + v_{i-1,j} - 2v_{i,j}}{\Delta x^2} + \frac{v_{i,j+1} + v_{i,j-1} - 2v_{i,j}}{\Delta y^2} \right) - \frac{P_{i,j} - P_{i,j-1}}{\Delta y}, \quad (7b)$$

$$0 = \frac{u_{i+1,j} - u_{i,j}}{\Delta x} + \frac{v_{i,j+1} - v_{i,j}}{\Delta y}. \quad (7c)$$

The boundary conditions for the velocity are given by the following equations

$$\begin{aligned} u_{i,j} &= u_b(x=0), \quad \frac{v_{i,j} + v_{i-1,j}}{2} = v_b(x=0), \quad \text{for } i=1, \\ u_{i,j} &= u_b(x=1), \quad \frac{v_{i,j} + v_{i-1,j}}{2} = v_b(x=1), \quad \text{for } i=nx+1, \\ \frac{u_{i,j} + u_{i,j-1}}{2} &= u_b(y=0), \quad v_{i,j} = v_b(y=0), \quad \text{for } j=1, \\ \frac{u_{i,j} + u_{i,j-1}}{2} &= u_b(y=1), \quad v_{i,j} = v_b(y=1), \quad \text{for } j=ny+1. \end{aligned} \quad (8)$$

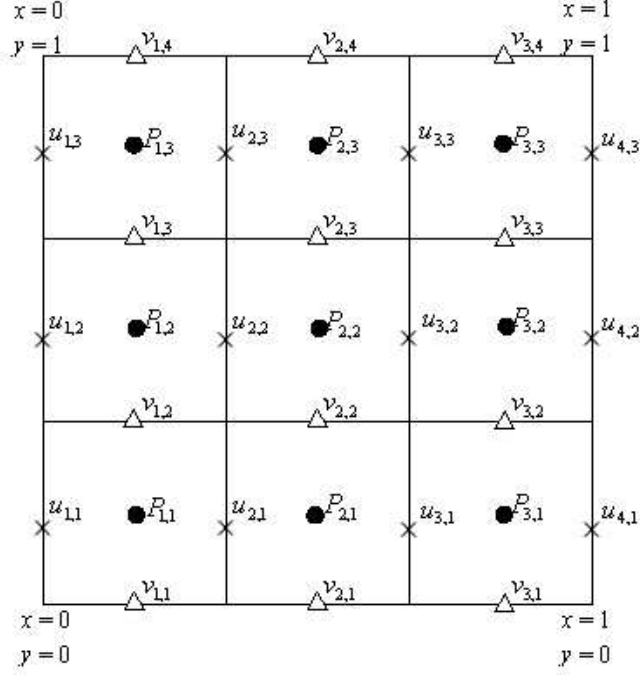


Figure 1: Spatial discretization (staggered grid).

No boundary conditions for pressure are needed since they are interior points. For the grid shown in Figure 1, we define the following velocity and pressure vectors for interior points only

$$u = [u_{2,1} \ u_{2,2} \ u_{2,3} \ u_{3,1} \ u_{3,2} \ u_{3,3} \ v_{1,2} \ v_{1,3} \ v_{2,2} \ v_{2,3} \ v_{3,2} \ v_{3,3}]^T, \quad (9)$$

$$P = [P_{1,1} \ P_{1,2} \ P_{1,3} \ P_{2,1} \ P_{2,2} \ P_{2,3} \ P_{3,1} \ P_{3,2} \ P_{3,3}]^T. \quad (10)$$

Using the boundary conditions (8), the matrices A , G and D can be written as

$$A = \begin{bmatrix} A_1 & 0 \\ 0 & A_2 \end{bmatrix}, \quad (11)$$

where

$$A_1 = \begin{bmatrix} -5 & 1 & 0 & 1 & 0 & 0 \\ 1 & -4 & 1 & 0 & 1 & 0 \\ 0 & 1 & -5 & 0 & 0 & 1 \\ 1 & 0 & 0 & -5 & 1 & 0 \\ 0 & 1 & 0 & 1 & -4 & 1 \\ 0 & 0 & 1 & 0 & 1 & -5 \end{bmatrix}, \quad A_2 = \begin{bmatrix} -5 & 1 & 1 & 0 & 0 & 0 \\ 1 & -5 & 0 & 1 & 0 & 0 \\ 1 & 0 & -4 & 1 & 1 & 0 \\ 0 & 1 & 1 & -4 & 0 & 1 \\ 0 & 0 & 1 & 0 & -5 & 1 \\ 0 & 0 & 0 & 1 & 1 & -5 \end{bmatrix}, \quad (12)$$

and

$$G = \begin{bmatrix} -1 & 0 & 0 & 1 & 0 & 0 & 0 & 0 & 0 \\ 0 & -1 & 0 & 0 & 1 & 0 & 0 & 0 & 0 \\ 0 & 0 & -1 & 0 & 0 & 1 & 0 & 0 & 0 \\ 0 & 0 & 0 & -1 & 0 & 0 & 1 & 0 & 0 \\ 0 & 0 & 0 & 0 & -1 & 0 & 0 & 1 & 0 \\ 0 & 0 & 0 & 0 & 0 & -1 & 0 & 0 & 1 \\ -1 & 1 & 0 & 0 & 0 & 0 & 0 & 0 & 0 \\ 0 & -1 & 1 & 0 & 0 & 0 & 0 & 0 & 0 \\ 0 & 0 & 0 & -1 & 1 & 0 & 0 & 0 & 0 \\ 0 & 0 & 0 & 0 & -1 & 1 & 0 & 0 & 0 \\ 0 & 0 & 0 & 0 & 0 & 0 & -1 & 1 & 0 \\ 0 & 0 & 0 & 0 & 0 & 0 & 0 & -1 & 1 \end{bmatrix}, \quad (13)$$

$$D = \begin{bmatrix} 1 & 0 & 0 & 0 & 0 & 0 & 1 & 0 & 0 & 0 & 0 & 0 \\ 0 & 1 & 0 & 0 & 0 & 0 & -1 & 1 & 0 & 0 & 0 & 0 \\ 0 & 0 & 1 & 0 & 0 & 0 & 0 & -1 & 0 & 0 & 0 & 0 \\ -1 & 0 & 0 & 1 & 0 & 0 & 0 & 0 & 1 & 0 & 0 & 0 \\ 0 & -1 & 0 & 0 & 1 & 0 & 0 & 0 & -1 & 1 & 0 & 0 \\ 0 & 0 & -1 & 0 & 0 & 1 & 0 & 0 & 0 & -1 & 0 & 0 \\ 0 & 0 & 0 & -1 & 0 & 0 & 0 & 0 & 0 & 0 & 1 & 0 \\ 0 & 0 & 0 & 0 & -1 & 0 & 0 & 0 & 0 & 0 & -1 & 1 \\ 0 & 0 & 0 & 0 & 0 & -1 & 0 & 0 & 0 & 0 & 0 & -1 \end{bmatrix}. \quad (14)$$

It is known and observed here that D and G are self-adjoint; i.e.,

$$D + G^T = 0. \quad (15)$$

It is well known that DG is the discretized Laplacian operator matrix, but it is singular. Actually it is the discretization of the following Poisson equation

$$\nabla^2 \phi = 0, \quad (16)$$

with boundary conditions

$$\frac{\partial \phi}{\partial \mathbf{n}} = 0.$$

We see that the solution of the above equation is not unique. Any solution plus a constant also satisfies the equation. This is corresponding to the singularity of matrix DG . We add an additional constraint to make the solution unique:

$$\sum_{i,j} \psi_{i,j} = 0, \quad (17)$$

where $\psi_{i,j}$ stands for the discrete unknowns in the grid points. Eq. (17) is equivalent to replace the

last row of DG with 1's, denoted as

$$L = \widehat{DG} = \begin{bmatrix} -2 & 1 & 0 & 1 & 0 & 0 & 0 & 0 & 0 \\ 1 & -3 & 1 & 0 & 1 & 0 & 0 & 0 & 0 \\ 0 & 1 & -2 & 0 & 0 & 1 & 0 & 0 & 0 \\ 1 & 0 & 0 & -3 & 1 & 0 & 1 & 0 & 0 \\ 0 & 1 & 0 & 1 & -4 & 1 & 0 & 1 & 0 \\ 0 & 0 & 1 & 0 & 1 & -3 & 0 & 0 & 1 \\ 0 & 0 & 0 & 1 & 0 & 0 & -2 & 1 & 0 \\ 0 & 0 & 0 & 0 & 1 & 0 & 1 & -3 & 1 \\ 1 & 1 & 1 & 1 & 1 & 1 & 1 & 1 & 1 \end{bmatrix}, \quad (18)$$

which is now invertible.

The underlying ODE

The mathematical structure of the DAE system (6) is referred to as Hessenberg index 2 [3]. In the DAE context, \mathbf{u} is the differential variable and P is the algebraic variable. The pressure P is further determined to be index 2, where the number of differentiations needed to determine the time derivative of P as a function of \mathbf{u} , P and t , is called the index of the DAE.

Defining $Q = GL^{-1}D$, both Q and $I - Q$ are projection operators, where I is the identity matrix. It is observed that

$$D(I - Q) = 0, \quad (19)$$

$$(I - Q)G = 0. \quad (20)$$

Multiplying Eq. (6a) by D from the left and using Eq. (6b), P can be solved as

$$P = L^{-1}DA\mathbf{u}. \quad (21)$$

Hence $GP = QA\mathbf{u}$, and we obtain the underlying ODE

$$\frac{d\mathbf{u}}{dt} = (I - Q)A\mathbf{u}, \quad (22)$$

which has the same solution as the DAE (6). Thus we can derive the analytical solution of the DAE (6) as a Taylor series,

$$\begin{aligned}
\mathbf{u}(t_{n+1}) &= \mathbf{u}(t_n) + \Delta t \left. \frac{d\mathbf{u}}{dt} \right|_{t_n} + \frac{\Delta t^2}{2} \left. \frac{d^2\mathbf{u}}{dt^2} \right|_{t_n} + \frac{\Delta t^3}{6} \left. \frac{d^3\mathbf{u}}{dt^3} \right|_{t_n} + \dots \\
&= \left(I + \Delta t(I - Q)A + \frac{\Delta t^2}{2} [(I - Q)A]^2 + \frac{\Delta t^3}{6} [(I - Q)A]^3 + \dots \right) \mathbf{u}(t_n),
\end{aligned} \tag{23}$$

and the analytical solution for $P(t_{n+1})$ is given by $GP(t_{n+1}) = QA\mathbf{u}(t_{n+1})$.

The idea of the projection method is first to get an intermediate solution, \mathbf{u}_{n+1}^* , by solving the following equation,

$$\frac{d\mathbf{u}^*}{dt} = A\mathbf{u}^* - Gq, \tag{24}$$

where q is an approximation of P . A straightforward choice for q is the pressure at the previous time step, P_n . Then a projection on \mathbf{u}_{n+1}^* is performed to get the solution \mathbf{u}_{n+1} which satisfies the constraint (6b).

The first projection

To obtain the numerical solution \mathbf{u}_{n+1} from the intermediate solution \mathbf{u}_{n+1}^* , the first projection is performed as follows

$$\phi_1 = L^{-1}D\mathbf{u}_{n+1}^*, \tag{25}$$

$$\mathbf{u}_{n+1} = \mathbf{u}_{n+1}^* - G\phi_1, \tag{26}$$

or simply written as $\mathbf{u}_{n+1} = (I - Q)\mathbf{u}_{n+1}^*$. The algebraic variable is updated as

$$P_{n+1}^{(1)} = q + \gamma \frac{\phi_1}{\Delta t}, \tag{27}$$

where Δt is the time step-size and γ is a coefficient to be determined, which will be discussed later. After the projection, \mathbf{u}_{n+1} satisfies the incompressibility constraint, i.e., $D\mathbf{u}_{n+1} = 0$ as well as $Q\mathbf{u}_{n+1} = 0$.

The additional projection

To obtain a more accurate pressure, we can perform an additional projection. The additional projection was first used in [32] to obtain a second-order approximation to the pressure. It involves implementing a hidden constraint, which can be derived by differentiating the incompressibility constraint (6b) with respect to time. This means $\mathbf{f} = \frac{d\mathbf{u}}{dt}$ should also satisfy the constraint (6b). Thus we have the following additional projection on \mathbf{f} ,

$$\phi_2 = L^{-1}D\mathbf{f}_{n+1}^*, \quad (28)$$

$$\mathbf{f}_{n+1} = \mathbf{f}_{n+1}^* - G\phi_2, \quad (29)$$

or simply $\mathbf{f}_{n+1} = (I - Q)\mathbf{f}_{n+1}^*$, where $\mathbf{f}_{n+1}^* = A\mathbf{u}_{n+1} - GP_{n+1}^{(1)}$. The algebraic variable is updated as

$$P_{n+1}^{(2)} = P_{n+1}^{(1)} + \phi_2. \quad (30)$$

Since

$$G\phi_2 = Q\mathbf{f}_{n+1}^* = QA\mathbf{u}_{n+1} - GP_{n+1}^{(1)}, \quad (31)$$

we have

$$GP_{n+1}^{(2)} = GP_{n+1}^{(1)} + G\phi_2 = QA\mathbf{u}_{n+1}, \quad (32)$$

or

$$Q(A\mathbf{u}_{n+1} - GP_{n+1}^{(2)}) = 0, \quad (33)$$

which says that $\mathbf{f}_{n+1} = A\mathbf{u}_{n+1} - GP_{n+1}^{(2)}$ satisfies the incompressibility constraint.

Clearly the additional projection enforces the incompressibility constraint for the acceleration $\mathbf{f} = \frac{d\mathbf{u}}{dt}$. And by doing that it brings the pressure to the same order of accuracy as the velocity as shown in Eq. (32). However, incorporating the additional projection into the pressure update in each time step may cause stability problems. Thus we use the additional projection as a post-processing step for output only. We will discuss this issue in Section 3.6. The additional projection

performed at the output is still a sufficient condition to obtain second-order accuracy in the pressure, provided that the velocity is second-order accurate. The additional projection can also be used in the initialization to obtain a consistent initial value for the pressure, starting from a consistent initial velocity.

It is noted that Klein and collaborators [24, 20] also use two projections for enforcing the incompressibility constraint when solving zero Froude number (incompressible) flow problems. However their two-projection method is quite different than our first and additional projection method. Their first and second projection are used to enforce the constraint on a Marker-and-cell (MAC) grid for advection velocity contribution and on the cell center for non-convective (e.g., pressure) contribution, respectively. In contrast our first and additional projection are enforcing the incompressibility constraint for the velocity and acceleration respectively. And the additional projection is performed only at the output when a second pressure is desired.

3 Projection Methods

We choose $\mathbf{q} = P_n$ in the projection methods. We obtain the first-order forward Euler and backward Euler projection methods when discretizing the time derivative in Eq. (24) using the forward Euler and backward Euler methods, respectively. We will focus on the second order projection methods, since they are the most often used. The methods below are all second order in the velocity. Depending on the form of the pressure update and the parameter γ , the pressure is either first-order or second-order accurate.

3.1 Second Order Projection Methods

3.1.1 Explicit Runge-Kutta second order method

It is possible to construct an explicit Runge-Kutta second order projection method by using the second-order Runge-Kutta method to integrate the momentum equation (24). The intermediate

solution is given by

$$\mathbf{u}_{n+1}^* = (I + \Delta t A + \frac{\Delta t^2}{2} A^2) \mathbf{u}_n - (\Delta t + \frac{\Delta t^2}{2} A) G P_n, \quad (34)$$

and

$$\begin{aligned} \mathbf{u}_{n+1} &= (I - Q) \mathbf{u}_{n+1}^*, \\ P_{n+1} &= P_n + \gamma \frac{\phi_1}{\Delta t}. \end{aligned}$$

Here, γ is a parameter which affects both order and stability, as will be discussed below.

3.1.2 Implicit trapezoidal method

We can also construct an implicit projection method by using the trapezoidal method to solve the momentum equation. Then the ODE (24) is discretized to

$$\frac{\mathbf{u}_{n+1}^* - \mathbf{u}_n}{\Delta t} = \frac{1}{2} A \mathbf{u}_{n+1}^* + \frac{1}{2} A \mathbf{u}_n - G P_n, \quad (35)$$

for which the solution is given by

$$\mathbf{u}_{n+1}^* = (I - \frac{1}{2} \Delta t A)^{-1} [(I + \frac{1}{2} \Delta t A) \mathbf{u}_n - \Delta t G P_n], \quad (36)$$

and

$$\begin{aligned} \mathbf{u}_{n+1} &= (I - Q) \mathbf{u}_{n+1}^*, \\ P_{n+1} &= P_n + \gamma \frac{\phi_1}{\Delta t}. \end{aligned}$$

We refer to this projection method as PM1.

If we perform the additional projection at every step in addition to PM1, according to the

analysis Eqs. (28)-(32), we obtain an “exact” pressure in the sense that P is proportional to \mathbf{u} , i.e., Eq. (32), which means P has the same order of accuracy as \mathbf{u} . We refer to this method as PM2. If we perform the additional projection only at the output in addition to PM1, we refer to this method as PM1B.

3.1.3 Runge-Kutta-Chebyshev projection method

The Runge-Kutta-Chebyshev projection (RKCP) method is a second order explicit Runge-Kutta type method, but with an extended stability region. It uses the Runge-Kutta-Chebyshev (RKC) method [29, 27, 30] to solve the ODE (6a). For details of the RKCP method, the reader is referred to [32].

The intermediate solution can be written as

$$\mathbf{u}_{n+1}^* = R(\Delta t A)\mathbf{u}_n - (R(\Delta t A) - I)A^{-1}GP_n, \quad (37)$$

where R is the stability polynomial of the RKC method. The solution is updated as

$$\begin{aligned} \mathbf{u}_{n+1} &= (I - Q)\mathbf{u}_{n+1}^*, \\ P_{n+1} &= P_n + \gamma \frac{\phi_1}{\Delta t}. \end{aligned}$$

The method can be used with the additional projection (for output purposes only), to obtain a second-order accurate pressure.

3.2 Common Framework

All of the above methods can be generalized to the following form. The intermediate solution is given by

$$\mathbf{u}_{n+1}^* = R(\Delta t A)\mathbf{u}_n - (R(\Delta t A) - I)A^{-1}GP_n, \quad (38)$$

where $R(\Delta t A)$ is the stability function of the corresponding ODE integration method. The solutions at the next step are updated as

$$\begin{aligned}\mathbf{u}_{n+1} &= (I - Q)\mathbf{u}_{n+1}^*, \\ P_{n+1} &= P_n + \gamma \frac{\phi_1}{\Delta t}.\end{aligned}\tag{39}$$

Different choices of $R(\Delta t A)$ yield different methods:

1. Forward Euler method, where $R(\Delta t A) = I + \Delta t A$.
2. Backward Euler method, where $R(\Delta t A) = (I - \Delta t A)^{-1}$.
3. Explicit Runge-Kutta second order method, where $R(\Delta t A) = I + \Delta t A + \frac{\Delta t^2}{2} A^2$.
4. Implicit trapezoidal method, where $R(\Delta t A) = (I - \frac{1}{2}\Delta t A)^{-1}(I + \frac{1}{2}\Delta t A)$.
5. Runge-Kutta-Chebyshev projection method, where R is the stability polynomial of the RKC method.

For second order projection methods, $R(\Delta t A)$ satisfies

$$R(\Delta t A) = I + \Delta t A + \frac{\Delta t^2}{2} A^2 + O(\Delta t^3).\tag{40}$$

It follows that

$$(R(\Delta t A) - I)A^{-1} = \Delta t I + \frac{\Delta t^2}{2} A + O(\Delta t^3).\tag{41}$$

In the following stability and order analysis, we will concentrate on the second order methods, since they are the main focus of this paper.

3.3 Stability Analysis

In this section we analyze the zero-stability and the absolute stability properties of the method consisting of (38) and (39).

Theorem 1. *Consider the system (6). If the ODE method defined via $R(\Delta t A)$ for $\frac{du}{dt} = Au$, where A is a symmetric matrix, is zero-stable, then the projection method (38)-(39) is zero-stable provided that $0 < \gamma \leq 2$. Furthermore, if the ODE method is absolutely stable for $\Delta t A$, then the projection method (38)-(39) is absolutely stable provided that $0 < \gamma \leq 2$.*

Proof. Using Eq. (38), the difference of the intermediate solutions, \mathbf{u}_{n+1}^* and \mathbf{u}_n^* is written as

$$\mathbf{u}_{n+1}^* - \mathbf{u}_n^* = R(\Delta t A)(\mathbf{u}_n - \mathbf{u}_{n-1}) - (R(\Delta t A) - I)A^{-1}G(P_n - P_{n-1}). \quad (42)$$

Since $P_n - P_{n-1} = \gamma \frac{\phi_1}{\Delta t}$, where $\phi_1 = L^{-1}D\mathbf{u}_n^*$, Eq. (42) is rewritten as

$$\mathbf{u}_{n+1}^* - \mathbf{u}_n^* = R(\Delta t A)(I - Q)(\mathbf{u}_n^* - \mathbf{u}_{n-1}^*) + (I - R(\Delta t A))\frac{\gamma}{\Delta t}A^{-1}Q\mathbf{u}_n^*. \quad (43)$$

Let $\mathbf{u}_n^* = \mathbf{v}_n + \mathbf{w}_n$, where $\mathbf{v}_n = (I - Q)\mathbf{u}_n^*$ and $\mathbf{w}_n = Q\mathbf{u}_n^*$. We rewrite Eq. (43) as

$$\mathbf{v}_{n+1} + \mathbf{w}_{n+1} - \mathbf{v}_n - \mathbf{w}_n = R(\Delta t A)(\mathbf{v}_n - \mathbf{v}_{n-1}) + (I - R(\Delta t A))\frac{\gamma}{\Delta t}A^{-1}\mathbf{w}_n. \quad (44)$$

Consider the following two recurrences:

$$v_{n+1} - v_n = R(\Delta t A)(v_n - v_{n-1}), \quad (45)$$

$$w_{n+1} = \left(I + (I - R(\Delta t A))\frac{\gamma}{\Delta t}A^{-1} \right) w_n. \quad (46)$$

The propagation matrices for the recurrences (45) and (46) are $R(\Delta t A)$ and $I + (I - R(\Delta t A))\frac{\gamma}{\Delta t}A^{-1}$ respectively. Letting $\Delta t \rightarrow 0$ in Eqs. (45) and (46) and considering Eqs. (40) and (41), zero-stability is easily established. For absolute stability, let $z = \Delta t \lambda_A$, where λ_A denotes an eigenvalue of A

Numerical Method	$R(z)$	Stability region $\ R(z)\ \leq 1$	$\frac{1-R(z)}{z}$
Forward Euler	$1 + z$	$\ 1 + z\ \leq 1$	-1
Backward Euler	$(1 + z)^{-1}$	$\ 1 - z\ \geq 1$	$-(1 - z)^{-1}$
Explicit RK2	$1 + z + \frac{z^2}{2}$	$\ 1 + z + \frac{z^2}{2}\ \leq 1$	$-(1 + \frac{z}{2})$
Implicit Trapezoidal	$(1 - \frac{z}{2})^{-1}(1 + \frac{z}{2})$	$Re(z) \leq 0$	$-(1 - \frac{z}{2})^{-1}$

Table 1: Stability polynomials $R(z)$

which is real because A is symmetric. So we consider z to be real and negative. It can be shown that for z in the stability region of the numerical ODE algorithm, i.e., $\|R(z)\| \leq 1$, we always have $-1 \leq \frac{1-R(z)}{z} \leq 0$ for the methods, as illustrated in Table 1.

It is clear that in order to make the recurrence (46) stable, we must choose $0 < \gamma \leq 2$. Now both recurrence (45) and recurrence (46) are stable. The sum of these two recurrences, Eq. (44), is therefore stable. \square

3.4 Order of Accuracy

Theorem 2. *Consider a projection method defined by Eqs. (38) and (39), where $0 < \gamma \leq 2$, R satisfies Eq. (40), and the initial values are chosen to be consistent. Then the method is convergent and second-order accurate in the velocities, and first-order accurate in the pressure. Furthermore, if $\gamma = 2$, the pressure is second-order accurate.*

Proof. Inserting Eqs. (40) and (41) into (38) and considering $Q\mathbf{u}_n = 0$, we find that

$$\begin{aligned}
Q\mathbf{u}_{n+1}^* &= QR(\Delta t A)\mathbf{u}_n - Q(R(\Delta t A) - I)A^{-1}GP_n \\
&= \Delta t Q(A\mathbf{u}_n - GP_n) + \frac{\Delta t^2}{2}QA(A\mathbf{u}_n - GP_n) + O(\Delta t^3),
\end{aligned} \tag{47}$$

and

$$\begin{aligned}
(I - Q)\mathbf{u}_{n+1}^* &= (I - Q)R(\Delta t A)\mathbf{u}_n - (I - Q)(R(\Delta t A) - I)A^{-1}GP_n \\
&= \mathbf{u}_n + \Delta t(I - Q)A\mathbf{u}_n + O(\Delta t^2) - \Delta t(I - Q)GP_n + O(\Delta t^2) \\
&= \mathbf{u}_n + \Delta t(I - Q)A\mathbf{u}_n + O(\Delta t^2).
\end{aligned} \tag{48}$$

Since

$$\begin{aligned}
A\mathbf{u}_{n+1} - GP_{n+1} &= A(I - Q)\mathbf{u}_{n+1}^* - G(P_n + \gamma \frac{\phi_1}{\Delta t}) \\
&= A\mathbf{u}_n + \Delta t A(I - Q)A\mathbf{u}_n + O(\Delta t^2) - GP_n - \gamma \frac{G\phi_1}{\Delta t},
\end{aligned} \tag{49}$$

and

$$\begin{aligned}
\frac{G\phi_1}{\Delta t} &= \frac{Q\mathbf{u}_{n+1}^*}{\Delta t} \\
&= Q(A\mathbf{u}_n - GP_n) + \frac{\Delta t}{2}QA(A\mathbf{u}_n - GP_n) + O(\Delta t^2),
\end{aligned} \tag{50}$$

we have

$$\begin{aligned}
Q(A\mathbf{u}_{n+1} - GP_{n+1}) &= (1 - \gamma)Q(A\mathbf{u}_n - GP_n) \\
&\quad + (1 - \frac{\gamma}{2})\Delta t QA(I - Q)A\mathbf{u}_n \\
&\quad - \frac{\gamma}{2}\Delta t QAQ(A\mathbf{u}_n - GP_n) + O(\Delta t^2).
\end{aligned} \tag{51}$$

We obtain the following recurrence

$$\mathbf{y}_{i+1} - \alpha \mathbf{y}_i = \Delta t \cdot \mathbf{g}(\mathbf{u}_i, P_i) + O(\Delta t^2), \quad i = 0, 1, \dots, n, \tag{52}$$

where

$$\begin{aligned}
\mathbf{y}_i &= Q(\mathbf{A}\mathbf{u}_i - GP_i), \\
\mathbf{g}(\mathbf{u}_i, P_i) &= (1 - \frac{\gamma}{2})QA(I - Q)\mathbf{A}\mathbf{u}_i \\
&\quad - \frac{\gamma}{2}QAQ(\mathbf{A}\mathbf{u}_i - GP_i), \\
\alpha &= 1 - \gamma.
\end{aligned}$$

Assuming $\|\mathbf{g}(\mathbf{u}_i, P_i)\| \leq C_1$, for $i = 0, 1, \dots, n$, and $\|O(\Delta t^2)\| \leq C_2\Delta t^2$, summation of the recurrence (52) multiplied by α^{n-i} from $i = 0$ to $i = n$ gives

$$\|\mathbf{y}_{n+1} - \alpha^{n+1}\mathbf{y}_0\| \leq \frac{1 - \alpha^{n+1}}{1 - \alpha}C_1\Delta t + \frac{1 - \alpha^{n+1}}{1 - \alpha}C_2\Delta t^2. \quad (53)$$

Since $0 < \gamma \leq 2$, we have $|\alpha| = |1 - \gamma| \leq 1$. Assuming that the initial values for \mathbf{u} and P are consistent, we have $\mathbf{y}_0 = 0$. Thus we arrive at

$$Q(\mathbf{A}\mathbf{u}_n - GP_n) = \mathbf{y}_n = O(\Delta t), \quad (54)$$

for any n , and

$$Q\mathbf{u}_{n+1}^* = O(\Delta t^2), \quad (55)$$

for any n , using Eq. (50). Eq. (54) establishes a global relationship between \mathbf{u}_n and P_n . From Eq. (54) we obtain

$$GP_n = Q\mathbf{A}\mathbf{u}_n + O(\Delta t). \quad (56)$$

Thus P is globally at least first-order accurate, given that \mathbf{u} is globally at least first-order accurate.

Using Eqs. (40) and (41), the numerical solution at time t_{n+1} is expanded as

$$\begin{aligned}
\mathbf{u}_{n+1} &= (I - Q)\mathbf{u}_{n+1}^* \\
&= \mathbf{u}_n + \Delta t(I - Q)A\mathbf{u}_n + \frac{\Delta t^2}{2}(I - Q)A^2\mathbf{u}_n \\
&\quad - \Delta t(I - Q)GP_n - \frac{\Delta t^2}{2}(I - Q)AGP_n + O(\Delta t^3) \\
&= \mathbf{u}_n + \Delta t(I - Q)A\mathbf{u}_n + \frac{\Delta t^2}{2}(I - Q)A^2\mathbf{u}_n \\
&\quad - \frac{\Delta t^2}{2}(I - Q)AGP_n + O(\Delta t^3).
\end{aligned} \tag{57}$$

According to Eq. (54), we have $GP_n = QA\mathbf{u}_n + O(\Delta t)$. Thus inequality (57) becomes

$$\mathbf{u}_{n+1} = \mathbf{u}_n + \Delta t(I - Q)A\mathbf{u}_n + \frac{\Delta t^2}{2}[(I - Q)A]^2\mathbf{u}_n + O(\Delta t^3). \tag{58}$$

Comparing Eq. (58) to the analytical solution, Eq. (23), we see that \mathbf{u} is locally second-order accurate. The choice of γ does not affect the accuracy of \mathbf{u} . Combined with the zero-stability shown in the previous section, \mathbf{u} is therefore second-order convergent.

We have shown that P is globally at least first-order accurate, given that \mathbf{u} is globally at least first-order accurate. P is globally second-order accurate when we start with a consistent initial condition and choose $\gamma = 2$. When $\gamma = 2$, $\mathbf{g}(\mathbf{u}_i, P_i)$ in Eq. (52) is

$$\mathbf{g}(\mathbf{u}_i, P_i) = -QA\mathbf{y}_i = O(\Delta t).$$

Thus $\|\mathbf{g}(\mathbf{u}_i, P_i)\| \leq C_1\Delta t$, $i = 0, 1, \dots, n$. Eq. (53) becomes

$$\|\mathbf{y}_{n+1} - \alpha^{n+1}\mathbf{y}_0\| \leq \frac{1 - \alpha^{n+1}}{1 - \alpha}C_1\Delta t^2 + \frac{1 - \alpha^{n+1}}{1 - \alpha}C_2\Delta t^2, \tag{59}$$

where $\alpha = 1 - \gamma = -1$. We obtain $\mathbf{y}_n = O(\Delta t^2)$. Thus P is globally second-order accurate, given that \mathbf{u} is globally second-order accurate. \square

The fact that the coefficient γ can be any number between 0 and 2 was first discovered

by Gresho [11, 13] and analyzed by Shen [25, 26] by demonstrating converged error estimates for $0 < \gamma \leq 2$. We derived the value of γ analytically and showed that the coefficient γ is independent of the order of accuracy of \mathbf{u} , but is restricted by the stability requirement. Furthermore, when $\gamma = 2$, PM1 is second-order convergent for both \mathbf{u} and P .

We can view the significance of γ from another point of view. For the projection method PM1, the intermediate solution is solved by Eq. (35), and the projection step can be written as

$$\frac{\mathbf{u}_{n+1} - \mathbf{u}_{n+1}^*}{\Delta t} = -\frac{G\phi_1}{\Delta t}. \quad (60)$$

Adding the above equation with Eq. (35) gives

$$\frac{\mathbf{u}_{n+1} - \mathbf{u}_n}{\Delta t} = \frac{1}{2}A\mathbf{u}_{n+1}^* + \frac{1}{2}A\mathbf{u}_n - GP_n - \frac{G\phi_1}{\Delta t}. \quad (61)$$

Eliminating ϕ_1 yields

$$\frac{\mathbf{u}_{n+1} - \mathbf{u}_n}{\Delta t} = \frac{1}{2}A\mathbf{u}_{n+1}^* + \frac{1}{2}A\mathbf{u}_n - \left(\left(1 - \frac{1}{\gamma}\right)GP_n + \frac{1}{\gamma}GP_{n+1}^{(1)} \right). \quad (62)$$

Clearly when $\gamma = 1$ it looks like a backward Euler method for the pressure. And when $\gamma = 2$ it looks like a trapezoidal method. Technically γ can be any number, but it is suggested to be $0 < \gamma \leq 2$ by the previous stability analysis. When γ is not 2, we will get a first-order accurate pressure $P_{n+1}^{(1)}$. But the second order accuracy can be easily recovered by performing the additional projection at the output as shown in Section 2.

3.5 Discussion of a Class of Projection Methods

A class of projection methods [7, 4, 5] for solving the incompressible Navier-Stokes equations is based on the following second-order, discrete form

$$\frac{\mathbf{u}_{n+1} - \mathbf{u}_n}{\Delta t} = \frac{1}{2}A\mathbf{u}_{n+1} + \frac{1}{2}A\mathbf{u}_n - GP_{n+\frac{1}{2}}, \quad (63)$$

which uses the trapezoidal method for the time discretization. Relating to our notation from Eq. (24), here q is set to be $P_{n-\frac{1}{2}}$. Thus the intermediate solution is given by

$$\frac{\mathbf{u}_{n+1}^* - \mathbf{u}_n}{\Delta t} = \frac{1}{2}A\mathbf{u}_{n+1}^* + \frac{1}{2}A\mathbf{u}_n - GP_{n-\frac{1}{2}}. \quad (64)$$

The pressure is updated as

$$P_{n+\frac{1}{2}} = P_{n-\frac{1}{2}} + \frac{\phi_1}{\Delta t}. \quad (65)$$

Alternatively, the pressure may be updated by

$$P_{n+\frac{1}{2}} = P_{n-\frac{1}{2}} + \frac{\phi_1}{\Delta t} - \frac{1}{2}A\phi_1, \quad (66)$$

which allows the pressure to retain second order accuracy [31, 7]. The projection method based on (66) is also known as the rotational pressure-correction scheme [28, 14].

A point to be noted is that the local truncation error of the trapezoidal method for Eq. (63) is [3]

$$-\frac{\Delta t^2}{12} \frac{d^3 \mathbf{u}}{dt^3} \Big|_{t_{n+\frac{1}{2}}} + O(\Delta t^4). \quad (67)$$

So we see the discrete equation (63) is second-order accurate for the velocity, but not necessarily for the pressure. However taking the divergence of Eq. (63) will eliminate the $O(\Delta t^2)$ term in the truncation error (67) and make it higher order $O(\Delta t^4)$, since $\frac{d^3 \mathbf{u}}{dt^3}$ is supposed to be divergence-free. Then the accurate pressure can be extracted from the resulting equation. Multiplying Eq. (63) by Q from the left, we obtain

$$GP_{n+\frac{1}{2}} = \frac{1}{2}QA\mathbf{u}_{n+1} + \frac{1}{2}QA\mathbf{u}_n. \quad (68)$$

A local order analysis of the above equation based on the analytical solution (23), assuming the velocities are accurate, reveals that the pressure is not locally second-order accurate. One can also use the following form of discretization

$$\frac{\mathbf{u}_{n+1} - \mathbf{u}_n}{\Delta t} = \frac{1}{2}A\mathbf{u}_{n+1} + \frac{1}{2}A\mathbf{u}_n - \frac{1}{2}(GP_{n+1} + GP_n), \quad (69)$$

in which the pressure is locally consistent to second order accuracy. The pressure update formula Eqs. (65) and (66) will be changed accordingly. We refer to the method of Eq. (63) with and without the pressure correction term $-\frac{1}{2}A\phi_1$ as PM4 and PM3 respectively. And we refer to the method of Eq. (69) with and without the pressure correction term $-\frac{1}{2}A\phi_1$ as PM4A and PM3A respectively.

The improved pressure update formula can be derived as follows. Subtracting Eq. (63) from Eq. (64) and considering $\mathbf{u}_{n+1}^* = \mathbf{u}_{n+1} + G\phi_1$, we have

$$GP_{n+\frac{1}{2}} = GP_{n-\frac{1}{2}} + \frac{1}{\Delta t}G\phi_1 - \frac{1}{2}AG\phi_1. \quad (70)$$

For Eq. (70) to be equivalent to Eq. (66), A and G must commute. We then multiply Eq. (70) by D from the left. After removing the singularity of DG as shown in Section 2, the resulting \widehat{DG} is invertible and then Eq. (66) follows. Alternatively we can derive from Eq. (70) that

$$(I - Q)AG\phi_1 = 0,$$

which implies that

$$AG\phi_1 = QAG\phi_1. \quad (71)$$

The condition of Eq. (71) or the commutativity of A and G is satisfied in the continuum limit of the incompressible Navier-Stokes equations, where A , corresponding to the Laplacian operator ∇^2 commutes with G , corresponding to the gradient operator ∇ . However, on a finite grid the discretized Laplacian operator A does not strictly commute with the discretized gradient operator G because of the spatial grid and the boundary conditions used. In this sense the rotational formula (66) may not be second-order accurate for problems where A and G do not commute. An exception is the case of periodic boundary conditions [17].

Brown *et al.* [7] have shown by normal mode analysis that the rotational projection methods (PM4 and PM4A) are temporally second-order accurate for the pressure, and it was observed in

numerical experiments [14, 22] that the pressure behaved as 1.6^{th} order or 2^{nd} order, depending on the problem. The analytical second order accuracy was obtained based on the assumption that A and G commute, which may not be strictly satisfied in practice. We speculate that this is the cause of the order reduction and the second-order accuracy is not guaranteed for the rotational method. Based on the condition that A and G commute, it is easy to show by local order analysis that PM4 and PM4A are locally second-order accurate for the pressure, following the same approach of Section 3.4. (See the Appendix for details.)

We can perform the additional projection for methods PM3 and PM4 at the output. These methods are referred to as PM3B and PM4B. As shown in Table 2 and Section 4, they are second-order accurate for the pressure. The specific projection methods that we consider here are summarized in Table 2.

3.6 Stability of Method PM2

When we use PM2 (Section 3.1.2), we obtain an accurate P satisfying $GP_n = QA\mathbf{u}_n$. Thus we can rewrite Eq. (38) as

$$\mathbf{u}_{n+1}^* = R(\Delta t A)\mathbf{u}_n - (R(\Delta t A) - I)A^{-1}QA\mathbf{u}_n. \quad (72)$$

It follows that

$$\mathbf{u}_{n+1} = T(\Delta t A)\mathbf{u}_n, \quad (73)$$

where

$$T(\Delta t A) = (I - Q)(R(\Delta t A) - (R(\Delta t A) - I)A^{-1}QA). \quad (74)$$

We see that $T(\Delta t A)$ is the stability polynomial of the projection method PM2 and $R(\Delta t A)$ is the stability polynomial of the ODE method for solving the intermediate velocity. For the implicit trapezoidal method, it is found that

$$T(\Delta t A) = (I - Q)\left(I - \frac{1}{2}\Delta t A\right)^{-1}\left(I + \frac{1}{2}\Delta t A - \Delta t QA\right). \quad (75)$$

Since A has negative eigenvalues, the term $-\Delta tQA$ will make $T(\Delta tA)$ less stable. For matrices (11)-(18), we can calculate the spectral radius of $R(\Delta tA)$, $(I - Q)R(\Delta tA)$ and $T(\Delta tA)$ for different Δt . As shown in Figure 2, it is found that the spectral radius of $T(\Delta tA)$ goes above 1 when Δt is greater than 6, meaning that the projection method PM2 does not preserve the unconditional stability of the implicit trapezoidal method.

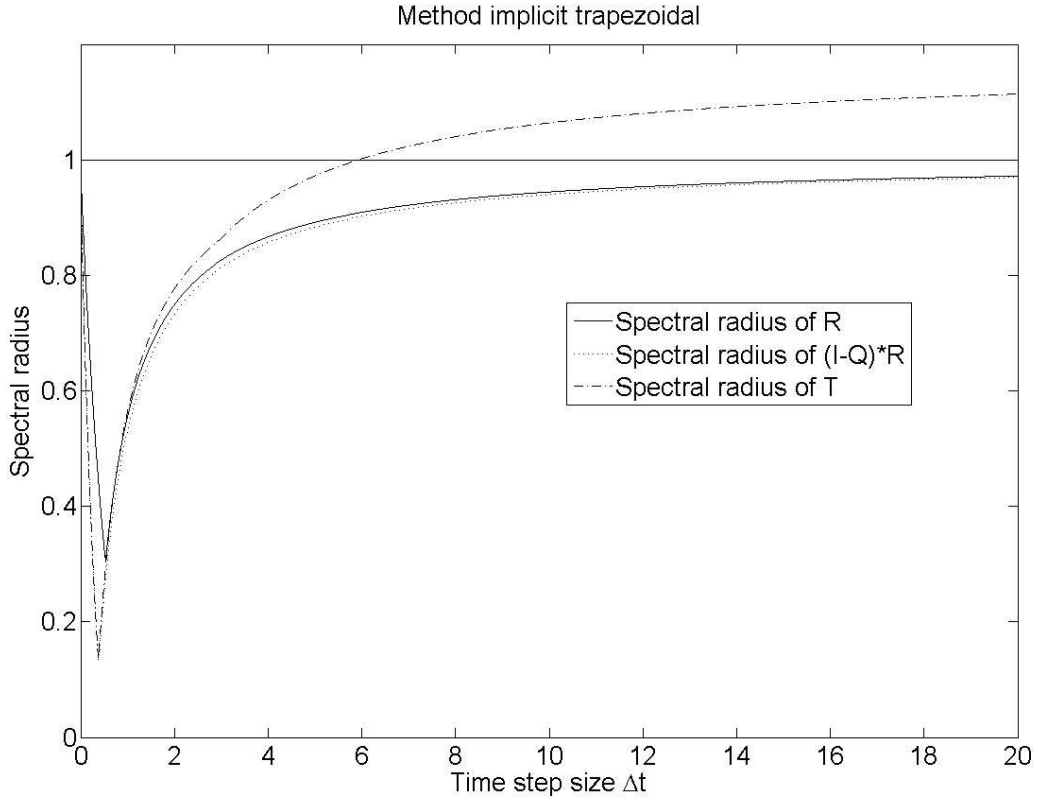


Figure 2: Stability shrinkage of PM2.

Remark

It is observed that PM2 preserves the stability in the special case where A and G commute. This is due to the fact that when A and G commute, any polynomial of A (e.g., $(R(\Delta tA) - I)A^{-1}$) also commutes with G . Thus we have

$$(I - Q)(R(\Delta tA) - I)A^{-1}GP_n = (I - Q)G(R(\Delta tA) - I)A^{-1}P_n = 0,$$

and Eq. (73) becomes

$$\mathbf{u}_{n+1} = (I - Q)R(\Delta t A)\mathbf{u}_n, \quad (76)$$

which has the same or smaller stability region as that of $R(\Delta t A)$.

3.7 Boundary Conditions

In this section we discuss the treatment of boundary conditions. We have been given boundary conditions for the velocity, $\mathbf{u}|_\Gamma = \mathbf{u}_b$. In the projection methods, since $\mathbf{u}_{n+1} = \mathbf{u}_{n+1}^* - G\phi_1$, the simplest choice of boundary conditions for the intermediate solution \mathbf{u}^* and projection correction ϕ_1 and ϕ_2 , respectively, is

$$\mathbf{u}_{n+1}^*|_\Gamma = \mathbf{u}_b, \quad (77)$$

and

$$\frac{\partial \phi_1}{\partial \mathbf{n}} \Big|_\Gamma = 0, \quad \frac{\partial \phi_2}{\partial \mathbf{n}} \Big|_\Gamma = 0. \quad (78)$$

The boundary condition on the pressure with one projection can be obtained from Eq. (39) as

$$\frac{\partial P_{n+1}}{\partial \mathbf{n}} \Big|_\Gamma = \frac{\partial P_n}{\partial \mathbf{n}} \Big|_\Gamma, \quad (79)$$

or

$$\frac{d}{dt} \left(\frac{\partial P}{\partial \mathbf{n}} \right) \Big|_\Gamma = 0. \quad (80)$$

This boundary condition gives only first-order accurate pressure. However in the additional projection, we enforce the boundary condition for $\mathbf{f} = \frac{d\mathbf{u}}{dt}$,

$$\mathbf{f}|_\Gamma = \frac{d\mathbf{u}_b}{dt}, \quad (81)$$

which is

$$\left(\frac{1}{Re} \nabla^2 \mathbf{u} - \nabla P \right) \Big|_\Gamma = \frac{d\mathbf{u}_b}{dt}, \quad (82)$$

in the continuous case. We see that the boundary condition for the pressure is implicitly implemented. For staggered grids the pressure variable is always in the interior of the domain and thus no boundary conditions are needed. However for nonstaggered grids, we do need to know the pressure value on the boundary. For example, in the nonstaggered grid discretization shown in Figure 3, when we evaluate $\frac{\partial P}{\partial x}$ at node (2,2) which is approximated by

$$\frac{P_{3,2} - P_{1,2}}{2\Delta x}, \quad (83)$$

we do not know the value of $P_{1,2}$. One option is to use the extrapolation $P_{1,2} = 2P_{2,2} - P_{3,2}$. Plugging it into Eq. (83) gives

$$\frac{P_{3,2} - P_{1,2}}{2\Delta x} = \frac{P_{3,2} - P_{2,2}}{\Delta x}, \quad (84)$$

which is actually the first order approximation of $\frac{\partial P}{\partial x}$ at node (2,2). The discretization of Eq. (6) on nonstaggered grids is written as

$$\frac{du_{i,j}}{dt} = \frac{1}{Re} \left(\frac{u_{i+1,j} + u_{i-1,j} - 2u_{i,j}}{\Delta x^2} + \frac{u_{i,j+1} + u_{i,j-1} - 2u_{i,j}}{\Delta y^2} \right) - \frac{P_{i+1,j} - P_{i-1,j}}{2\Delta x}, \quad (85a)$$

$$\frac{dv_{i,j}}{dt} = \frac{1}{Re} \left(\frac{v_{i+1,j} + v_{i-1,j} - 2v_{i,j}}{\Delta x^2} + \frac{v_{i,j+1} + v_{i,j-1} - 2v_{i,j}}{\Delta y^2} \right) - \frac{P_{i,j+1} - P_{i,j-1}}{2\Delta y}, \quad (85b)$$

$$0 = \frac{u_{i+1,j} - u_{i-1,j}}{2\Delta x} + \frac{v_{i,j+1} - v_{i,j-1}}{2\Delta y}. \quad (85c)$$

The boundary conditions are given by

$$\begin{aligned} u_{i,j} &= u_b(x=0), \quad v_{i,j} = v_b(x=0), \quad P_{i,j} = 2P_{i+1,j} - P_{i+2,j}, \quad \text{for } i = 1, \\ u_{i,j} &= u_b(x=1), \quad v_{i,j} = v_b(x=1), \quad P_{i,j} = 2P_{i-1,j} - P_{i-2,j}, \quad \text{for } i = nx, \\ u_{i,j} &= u_b(y=0), \quad v_{i,j} = v_b(y=0), \quad P_{i,j} = 2P_{i,j+1} - P_{i,j+2}, \quad \text{for } j = 1, \\ u_{i,j} &= u_b(y=1), \quad v_{i,j} = v_b(y=1), \quad P_{i,j} = 2P_{i,j-1} - P_{i,j-2}, \quad \text{for } j = ny. \end{aligned} \quad (86)$$

Similar to the analysis in Section 2, we evaluate the matrices for interior nodes only. With non-staggered discretization (85) and (86), we found that $D + G^T \neq 0$ and $D(I - Q) \neq 0$ which means

that the projected velocity is not divergence free. Our stability and order analysis does not apply in this case, because it is based on the properties of Eqs. (19) and (20). And it is observed by numerical experiments that the above nonstaggered discretization causes an instability for method PM1 when $\gamma = 2$. This is possibly due to the fact that the nonstaggered discretization generates an expanded five-point stencil which produces a local decoupling of the mesh points and causes additional numerical difficulties, as mentioned in [1].

However, if we define the new divergence matrix as

$$\tilde{D} = -G^T, \quad (87)$$

then the properties Eqs. (19) and (20) are satisfied again. Numerical experiments show that for this choice of discretized divergence matrix, PM1 with $\gamma = 2$ is stable and second-order accurate for both velocity and pressure, as the analysis predicts. With this new “divergence” matrix, the incompressibility is not strictly satisfied near the boundary. Thus the idea here is similar to the approximate projection methods [2, 1] in that numerical difficulties are circumvented by relaxing the incompressibility constraint in some way. We note that this modification of the divergence matrix produces a local coupling of mesh points near the boundary.

4 Numerical Experiments

Following the analysis of [22], the numerical solution obtained by a method which is r -th order accurate in time and s -th order accurate in space can be expressed as

$$\eta_{i,j}^n = \eta(x_i, y_j, t^n) + \alpha_{i,j}^n (\Delta t)^r + \beta_{i,j}^n (\Delta x)^s + \epsilon, \quad (88)$$

where $\eta_{i,j}^n$ is the numerical solution at (x_i, y_j, t^n) , $\eta(x_i, y_j, t^n)$ is the reference solution, $\alpha_{i,j}^n (\Delta t)^r$ represents the error associated with the temporal discretization, $\beta_{i,j}^n (\Delta x)^s$ represents the error associated with the spatial discretization and ϵ is the round-off error. To check the temporal convergence,

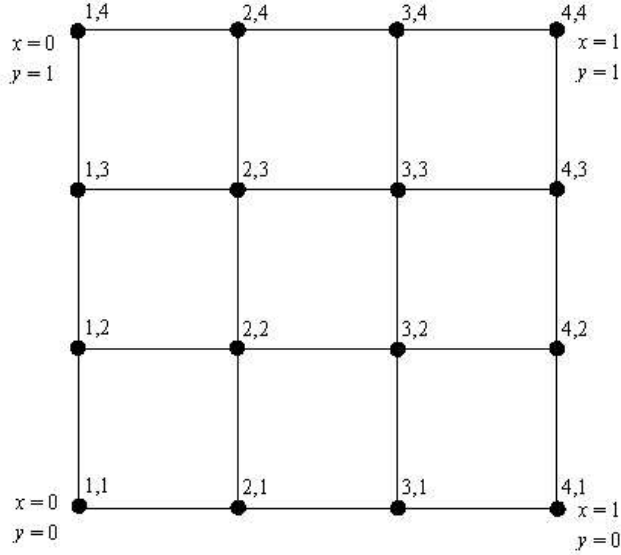


Figure 3: Spatial discretization (nonstaggered grid).

we fix the spatial grid and then compute a reference solution which is obtained using a very small time step ($\Delta t \ll 1$) so that the term $\alpha_{i,j}^n (\Delta t)^r$ can be ignored. The temporally accurate reference solution is approximately

$$\tilde{\eta}_{i,j}^n = \eta(x_i, y_j, t^n) + \beta_{i,j}^n (\Delta x)^s + \epsilon. \quad (89)$$

Then $\|\eta^n - \tilde{\eta}^n\| \sim (\Delta t)^r$. A plot of $\log(\|\eta^n - \tilde{\eta}^n\|)$ vs $\log(\Delta t)$ gives the information of the order r . Similarly, for the spatial convergence we fix the time step and compute the reference solution using a very small Δx . The spatially accurate reference solution is approximately

$$\hat{\eta}_{i,j}^n = \eta(x_i, y_j, t^n) + \alpha_{i,j}^n (\Delta t)^r + \epsilon. \quad (90)$$

Thus we have $\|\eta^n - \hat{\eta}^n\| \sim (\Delta x)^s$. A plot of $\log(\|\eta^n - \hat{\eta}^n\|)$ vs $\log(\Delta x)$ yields the order of spatial convergence. In the following tests, all the temporally accurate reference solutions, \mathbf{u}_0 and P_0 , were computed with $\Delta t = 1.0 \times 10^{-5}$.

The first numerical example is a forced flow problem. In this forced flow problem, the exact solution of the Navier-Stokes equations is given by

$$\begin{aligned}
u(x, y, t) &= \sin(t)\sin^2(\pi x)\sin(2\pi y), \\
v(x, y, t) &= -\sin(t)\sin(2\pi x)\sin^2(\pi y), \\
P(x, y, t) &= \sin(t)\cos(\pi x)\sin(\pi y),
\end{aligned} \tag{91}$$

with appropriate forcing terms added to the incompressible Navier-Stokes equations (1) to ensure that (91) is the exact solution. We solved this problem in the domain $[0, 1] \times [0, 1]$ to the time $T = 1s$ with Reynolds number $Re = 1$. Dirichlet boundary conditions were applied for both u and v .

The second numerical example is the driven cavity problem. In this test we solved the driven cavity problem in the domain $[0, 1] \times [0, 1]$ to the time $T = 1s$ with Reynolds number $Re = 100$. Zero Dirichlet boundary conditions were applied for the velocities, except that on the top boundary $y = 1$, the x -direction velocity u was set to 1. The initial velocity was set to 0 and the initial pressure was corrected from the initial guess 0 by performing the additional projection so that the initial pressure is consistent with the initial velocity.

All the tests have been completed on 64×64 staggered grids. We also did the tests on nonstaggered grids for projection method PM1 and PM1B.

All the methods tested here give second-order accuracy for the velocity. As shown in Figure 4, PM1 with $\gamma = 1$ is first-order accurate for the pressure in general, while PM1 with $\gamma = 2$ gives second-order accurate pressure. However method PM1B, i.e., PM1 plus an additional projection at the output, is also second-order accurate for the pressure and is more robust with a smaller error level for the pressure.

From Figure 5, we saw only first-order convergence for the pressure with methods PM3 and PM4. In the modified version of PM3 and PM4, i.e., PM3A and PM4A, we observed $1.6^{th} \sim 1.7^{th}$ order convergence for the forced flow problem and 2^{nd} order convergence for the driven cavity problem. The methods PM3 and PM4 can be improved by performing the additional projection at the output, which are methods PM3B and PM4B. They give no worse or better accuracy for the

pressure.

The results of the temporal order of the pressure are summarized in Table 2. The orders of the velocity are neglected in Table 2 since all of them are around 2 (± 0.1). The results shown here are consistent with the analysis. In short we recommend method PM1B for practical use, because it gives second-order accuracy for both the velocity and the pressure and is very robust.

5 Conclusions

In this paper we explored two types of projection: the first projection on the velocity, and the additional projection on the acceleration. These projections enforce the incompressibility constraint and the hidden constraint (time derivative of the incompressibility constraint), respectively. We proposed a common framework for projection methods based on the DAE structure Eq. (6) and we performed an analysis of accuracy and stability. With the additional projection performed at the output, we are able to get second-order accuracy for both velocity and pressure. The additional projection can also be used in the initialization to get the consistent initial value for the pressure. We addressed some issues related to the pressure update: how it affects the temporal order and stability, and explained some observations about the pressure-update coefficient γ that have been reported in the literature. We derived the conditions on the parameter γ and found that these conditions represent a stability requirement.

In particular, we proposed the implicit trapezoidal projection method PM1B. In this method, one projection of the velocity is performed per step and an additional projection is performed at the output of the solution to get a second-order accurate pressure. This method, robust and easy to implement, allows both the velocity and the pressure to be accurately calculated to second-order accuracy. It does not require complex boundary conditions. Simple boundary conditions are used for the intermediate velocity and the projection correction. We analyzed the order and stability for PM1B and showed theoretically that it is second-order convergent for both the velocity and the pressure, consistent with the numerical results we have obtained.

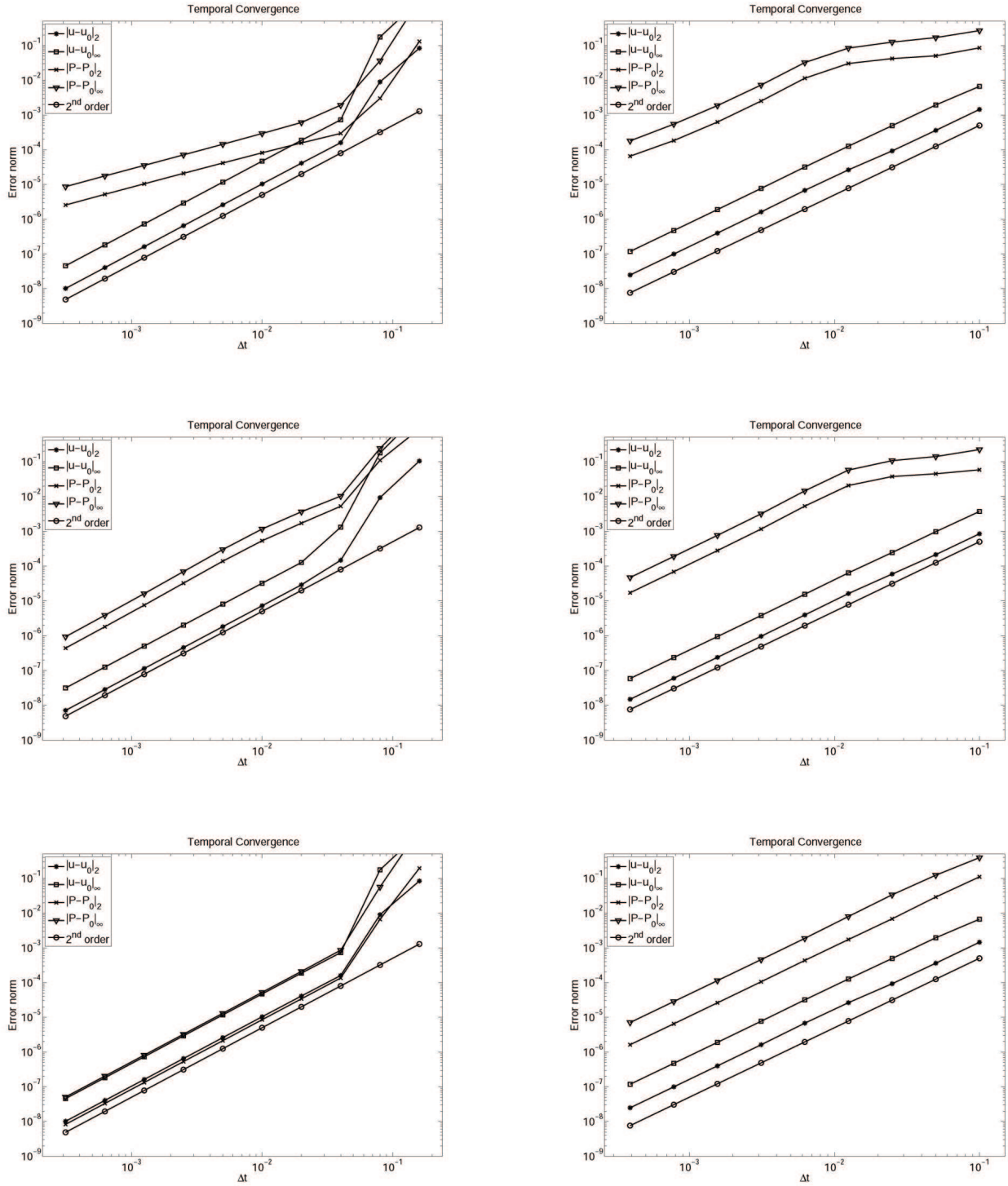


Figure 4: Error plots for projection method PM1. Left (driven cavity problem on staggered grids): top – PM1 with $\gamma = 1$; middle – PM1 with $\gamma = 2$; bottom – PM1B. Right (Force flow problem on nonstaggered grids): top – PM1 with $\gamma = 1$; middle – PM1 with $\gamma = 2$; bottom – PM1B.

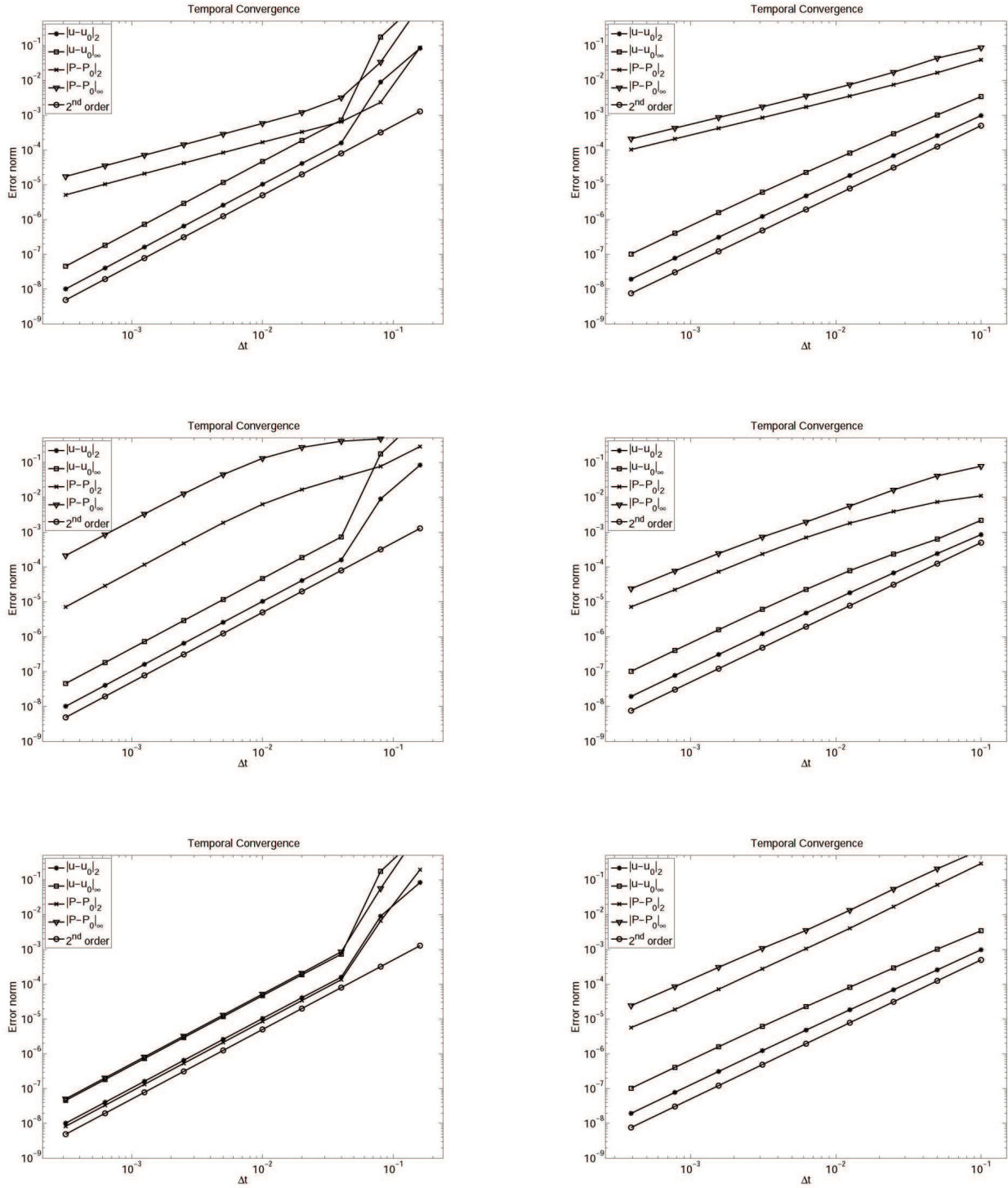


Figure 5: Error plots for projection methods PM3 and PM4. Left (driven cavity problem on staggered grids): top – PM3; middle – PM3A; bottom – PM3B. Right (Force flow problem on staggered grids): top – PM4; middle – PM4A; bottom – PM4B.

We also discussed a class of projection methods: the standard form and the rotational form, i.e., PM3 and PM4, and their slightly modified versions PM3A and PM4A. While only first order convergence for the pressure was observed for PM3 and PM4, $1.6^{th} \sim 2^{nd}$ order convergence for the pressure was observed for PM3A and PM4A, depending on the problem. The analysis as well as numerical experiments suggests that the rotational pressure update formula (66) may not be a sufficient condition for the pressure to be temporally second-order accurate. Although the rotational form does help reduce the pressure error at the boundary as discovered in [14], in our tests the rotational form exhibits the same order of accuracy as the standard form. We believe this may be due to the noncommutativity of the discretized Laplacian operator and the discretized gradient operator.

The additional projection, performed at the output, can be applied in all the projection methods which give second-order accurate velocity but first-order accurate pressure, to improve the pressure accuracy to be second order. As demonstrated by analysis and by numerical examples in this paper, it works for methods PM1, PM3 and PM4.

We also explained the stability issues with the method PM2, in which both the first projection and the additional projection are performed at each time step.

Acknowledgement

We would like to thank the referees for several illuminating comments.

Projection Method	Description	Grid	Theoretical order of P^1	Observed order of P		Preserve the stability of $R(\Delta t A)$
				Forced flow problem	Driven cavity problem	
PM1	$q = P_n$ Eq. (35)	Staggered	$2, \gamma = 2$ $1, 0 < \gamma < 2$	$2.00, \gamma = 2$ $1.04, \gamma = 1$	$2.05, \gamma = 2$ $1.02, \gamma = 1$	Yes, if $0 < \gamma \leq 2$
		Nonstaggered	$2, \gamma = 2$ $1, 0 < \gamma < 2$	$2.01, \gamma = 2$ $1.63, \gamma = 1$	N/A	Yes, if $0 < \gamma \leq 2$
PM1B	PM1 + additional projection at output only	Staggered	2	2.00	2.00	Yes, if $0 < \gamma \leq 2$
		Nonstaggered	2	2.00	1.99	Yes, if $0 < \gamma \leq 2$
PM2	PM1 + additional projection per step	Staggered	2	2.01	2.00	No
PM3	$q = P_{n-\frac{1}{2}}$ Eqs. (64) and (65)	Staggered	1	1.03	1.02	Yes
PM3A	$q = \frac{1}{2}(P_{n-1} + P_n)$ Eqs. (64) and (65)	Staggered	1	1.77	2.01	Yes
PM3B	PM3 (or PM3A) + additional projection at output only	Staggered	2	2.00	2.00	Yes
PM4	$q = P_{n-\frac{1}{2}}$ Eqs. (64) and (66)	Staggered	1	1.02	1.02	Yes
PM4A	$q = \frac{1}{2}(P_{n-1} + P_n)$ Eqs. (64) and (66)	Staggered	1	1.67	2.03	Yes
PM4B	PM4 (or PM4A) + additional projection at output only	Staggered	2	1.83	2.00	Yes

Table 2: Summary of projection methods

¹The theoretical order of P is obtained based on the condition that A and G do not commute.

Appendix

The discrete equation for the projection method PM4 is given by

$$\frac{\mathbf{u}_{n+1} - \mathbf{u}_n}{\Delta t} = \frac{1}{2}A\mathbf{u}_{n+1} + \frac{1}{2}A\mathbf{u}_n - GP_{n+\frac{1}{2}}, \quad (92)$$

the intermediate solution is given by

$$\frac{\mathbf{u}_{n+1}^* - \mathbf{u}_n}{\Delta t} = \frac{1}{2}A\mathbf{u}_{n+1}^* + \frac{1}{2}A\mathbf{u}_n - GP_{n-\frac{1}{2}}, \quad (93)$$

and the pressure is updated as

$$P_{n+\frac{1}{2}} = P_{n-\frac{1}{2}} + \frac{\phi_1}{\Delta t} - \frac{1}{2}A\phi_1. \quad (94)$$

We assume \mathbf{u}_n and $P_{n-\frac{1}{2}}$ are accurate. So \mathbf{u}_n is divergence free, i.e., $Q\mathbf{u}_n = 0$, and $GP_{n-\frac{1}{2}}$ can be written as

$$GP_{n-\frac{1}{2}} = QA\mathbf{u}(t_{n-\frac{1}{2}}) = QA\mathbf{u}_n - \frac{\Delta t}{2}QA(I-Q)A\mathbf{u}_n + \frac{\Delta t^2}{8}QA[(I-Q)A]^2\mathbf{u}_n + O(\Delta t^3). \quad (95)$$

From Eq. (93), \mathbf{u}_{n+1}^* can be solved as

$$\mathbf{u}_{n+1}^* = \left[I - \frac{1}{2}\Delta t A \right]^{-1} \left[\left(I + \frac{1}{2}\Delta t A \right) \mathbf{u}_n - \Delta t GP_{n-\frac{1}{2}} \right]. \quad (96)$$

Since

$$\left(I - \frac{1}{2}\Delta t A \right)^{-1} = I + \frac{1}{2}\Delta t A + \frac{1}{4}\Delta t^2 A^2 + \frac{1}{8}\Delta t^3 A^3 + O(\Delta t^4), \quad (97)$$

and

$$\left(I - \frac{1}{2}\Delta t A \right)^{-1} \left(I + \frac{1}{2}\Delta t A \right) = I + \Delta t A + \frac{1}{2}\Delta t^2 A^2 + \frac{1}{4}\Delta t^3 A^3 + O(\Delta t^4), \quad (98)$$

Eq. (96) becomes

$$\begin{aligned}\mathbf{u}_{n+1}^* &= (I + \Delta t A + \frac{1}{2}\Delta t^2 A^2 + \frac{1}{4}\Delta t^3 A^3)\mathbf{u}_n \\ &\quad - (I + \frac{1}{2}\Delta t A + \frac{1}{4}\Delta t^2 A^2)\Delta t GP_{n-\frac{1}{2}} + O(\Delta t^4).\end{aligned}\tag{99}$$

Using Eq. (95), we can get

$$\begin{aligned}\frac{G\phi_1}{\Delta t} &= \frac{Q\mathbf{u}_{n+1}^*}{\Delta t} \\ &= \Delta t QA(I - Q)A\mathbf{u}_n + \frac{1}{4}\Delta t^2 QA(I + Q)A(I - Q)A\mathbf{u}_n \\ &\quad - \frac{1}{8}\Delta t^2 QA[(I - Q)A]^2 \mathbf{u}_n + O(\Delta t^3).\end{aligned}\tag{100}$$

Therefore, adding Eqs. (95) and (100), we see that

$$\begin{aligned}GP_{n-\frac{1}{2}} + \frac{G\phi_1}{\Delta t} \\ = QA\mathbf{u}_n + \frac{1}{2}\Delta t QA(I - Q)A\mathbf{u}_n + \frac{1}{4}\Delta t^2 QA(I + Q)A(I - Q)A\mathbf{u}_n + O(\Delta t^3)\end{aligned}\tag{101}$$

is locally first-order accurate to the analytical solution $GP(t_n + \frac{1}{2})$, which can be calculated from Eq. (23).

Using the property that G and A commute, we have

$$GA\phi_1 = QGA\phi_1 = QAG\phi_1 = \Delta t^2 QAQA(I - Q)A\mathbf{u}_n + O(\Delta t^3).\tag{102}$$

We then get

$$\begin{aligned}GP_{n-\frac{1}{2}} + \frac{G\phi_1}{\Delta t} - \frac{1}{2}GA\phi_1 \\ = QA\mathbf{u}_n + \frac{1}{2}\Delta t QA(I - Q)A\mathbf{u}_n + \frac{1}{4}\Delta t^2 QA[(I - Q)A]^2 \mathbf{u}_n + O(\Delta t^3),\end{aligned}\tag{103}$$

which is locally second-order accurate to $GP(t_n + \frac{1}{2})$.

The discrete equation for the projection method PM4A is given by

$$\frac{\mathbf{u}_{n+1} - \mathbf{u}_n}{\Delta t} = \frac{1}{2}A\mathbf{u}_{n+1} + \frac{1}{2}A\mathbf{u}_n - \frac{1}{2}(GP_{n+1} + GP_n), \quad (104)$$

the intermediate solution is given by

$$\frac{\mathbf{u}_{n+1}^* - \mathbf{u}_n}{\Delta t} = \frac{1}{2}A\mathbf{u}_{n+1}^* + \frac{1}{2}A\mathbf{u}_n - \frac{1}{2}(GP_n + GP_{n-1}), \quad (105)$$

and the pressure is updated as

$$\frac{1}{2}(P_{n+1} + P_n) = \frac{1}{2}(P_n + P_{n-1}) + \frac{\phi_1}{\Delta t} - \frac{1}{2}A\phi_1, \quad (106)$$

or

$$P_{n+1} = P_{n-1} + \frac{2\phi_1}{\Delta t} - A\phi_1. \quad (107)$$

Assuming \mathbf{u}_n , P_n and P_{n-1} are accurate, we have $Q\mathbf{u}_n = 0$, $GP_n = Q\mathbf{A}\mathbf{u}_n$ and

$$GP_{n-1} = Q\mathbf{A}\mathbf{u}(t_{n-1}) = Q\mathbf{A}\mathbf{u}_n - \Delta tQA(I - Q)\mathbf{A}\mathbf{u}_n + \frac{\Delta t^2}{2}QA[(I - Q)A]^2\mathbf{u}_n + O(\Delta t^3). \quad (108)$$

From Eq. (105), \mathbf{u}_{n+1}^* is solved as

$$\mathbf{u}_{n+1}^* = \left[I - \frac{1}{2}\Delta tA \right]^{-1} \left[\left(I + \frac{1}{2}\Delta tA \right)\mathbf{u}_n - \frac{\Delta t}{2}(GP_n + GP_{n-1}) \right]. \quad (109)$$

Using Eqs. (97), (98) and (108), we can derive that

$$\begin{aligned} \frac{G\phi_1}{\Delta t} &= \frac{Q\mathbf{u}_{n+1}^*}{\Delta t} \\ &= \Delta tQA(I - Q)\mathbf{A}\mathbf{u}_n + \frac{1}{2}\Delta t^2QAQA(I - Q)\mathbf{A}\mathbf{u}_n + O(\Delta t^3). \end{aligned} \quad (110)$$

Similar to PM4, $GP_{n-1} + \frac{2G\phi_1}{\Delta t}$ is locally first-order accurate to the analytical solution $GP(t_n + 1)$,

and

$$\begin{aligned}
& GP_{n-1} + \frac{2G\phi_1}{\Delta t} - GA\phi_1 \\
& = QAU_n + \Delta tQA(I - Q)AU_n + \frac{1}{2}\Delta t^2QA[(I - Q)A]^2\mathbf{u}_n + O(\Delta t^3)
\end{aligned} \tag{111}$$

is locally second-order accurate to $GP(t_n + 1)$.

References

- [1] A.S. Almgren, J.B. Bell, and W.Y. Crutchfield. Approximate projection methods: Part I. Inviscid analysis. *SIAM J. Sci. Comput.*, 22:1139, 2000.
- [2] A.S. Almgren, J.B. Bell, and W.G. Szymczak. A numerical method for the incompressible Navier-Stokes equations based on an approximate projection. *SIAM J. Sci. Comput.*, 17:358, 1996.
- [3] U.M. Ascher and L.R. Petzold. *Computer methods for ordinary differential equations and differential-algebraic equations*. Society for Industrial and Applied Mathematics, 1998.
- [4] J.B. Bell, P. Colella, and H.M. Glaz. A second order projection method for the incompressible Navier-Stokes equations. *J. Comp. Phys.*, 85:257, 1989.
- [5] J.B. Bell, P. Colella, and L.H. Howell. An efficient second-order projection method for viscous incompressible flow. In *Proceedings of the Tenth AIAA Computational Fluid Dynamics Conference*, page 360. AIAA, 1991.
- [6] O. Botella. On the solution of the Navier-Stokes equations using Chebyshev projection schemes with third-order accuracy in time. *Computers and Fluids*, 26:107, 1997.
- [7] D.L. Brown, R. Cortez, and M.L. Minion. Accurate projection methods for the incompressible Navier-Stokes equations. *J. Comp. Phys.*, 168:464, 2001.

- [8] A.J. Chorin. Numerical solution of the Navier-Stokes equations. *Math. Comp.*, 22(104):745, 1968.
- [9] A.J. Chorin. On the convergence of discrete approximation to the Navier-Stokes equations. *Math. Comput.*, 23:341, 1969.
- [10] W. E and J.G. Liu. Gauge method for viscous incompressible flows. *Comm. Math. Sci.*, 1:317, 2003.
- [11] P.M. Gresho. On the theory of semi-implicit projection methods for viscous incompressible flow and its implementation via a finite element method that also introduces a nearly consistent mass matrix. Part 1: theory. *Int. J. Numer. Meth. Fluids*, 11:587, 1990.
- [12] P.M. Gresho and R.L. Sani. On pressure boundary conditions for the incompressible Navier-Stokes equations. *Int. J. Numer. Meth. Fluids*, 7:1111, 1987.
- [13] P.M. Gresho and R.L. Sani. *Incompressible flow and the finite element method. Volume two: isothermal laminar flow*. John Wiley & Sons Ltd, 1998.
- [14] J.L. Guermond, P. Mineev, and J. Shen. An overview of projection methods for incompressible flows. *Comput. Methods Appl. Mech. Engrg.*, 195:6011, 2006.
- [15] J.L. Guermond and L. Quartapelle. On stability and convergence of projection methods based on pressure Poisson equation. *Int. J. Numer. Meth. Fluids*, 26:1039, 1998.
- [16] R.D. Guy and A.L. Fogelson. Stability of approximate projection methods on cell-centered grids. *J. Comp. Phys.*, 203:517, 2005.
- [17] J.B. Perot. An analysis of the fractional step method. *J. Comp. Phys.*, 108:51, 1993.
- [18] J.K. Dukowicz and A.S. Dvinsky. Approximate factorization as a high order splitting for the implicit incompressible flow equations. *J. Comp. Phys.*, 102:336, 1992.

- [19] J.Kim and P. Moin. Application of a fractional-step method to incompressible Navier-Stokes equations. *J. Comp. Phys.*, 59:308, 1985.
- [20] S.Y. Kadioglu, R. Klein, and M.L. Minion.
- [21] J.V. Kan. A second-order accurate pressure-correction scheme for viscous incompressible flow. *SIAM J. Sci. Stat. Comput.*, 7:871, 1986.
- [22] M. Liu, Y. Ren, and H. Zhang. A class of fully second order accurate projection methods for solving the incompressible Navier-Stokes equations. *J. Comp. Phys.*, 200:325, 2004.
- [23] R. Témam. Sur l'approximation de la solution des équations de navier-stokes par la méthode des pas fractionnaires (ii). *Arch. Rat. Mech. Anal.*, 33:377, 1969.
- [24] S. Vater and R. Klein. Stability of a Cartesian grid projection method for zero Froude number shallow water flows. *ZIB Report 07-13, Konrad-Zuse-Zentrum für Informationstechnik Berlin*, 2007.
- [25] J. Shen. On error estimates of some higher order projection and penalty-projection methods for Navier-Stokes equations. *Numer. Math.*, 62:49, 1992.
- [26] J. Shen. On error estimates of the projection methods for the Navier-Stokes equations: Second order schemes. *Math. Comput.*, 65(215):1039, 1996.
- [27] B.P. Sommeijer, L.F. Shampine, and J.G. Verwer. RKC: an explicit solver for parabolic PDEs. *J. Comp. Appl. Math.*, 88:315, 1997.
- [28] L.J.P. Timmermans, P.D. Mineev, and F.N. Van De Vosse. An approximate projection scheme for incompressible flow using spectral elements. *Int. J. Numer. Meth. Fluids*, 22:673, 1996.
- [29] P.J. van der Houwen and B.P. Sommeijer. On the internal stability of explicit, m -stage Runge-Kutta methods for large m -values. *Z. Angew. Math. Mech.*, 60:479, 1980.

- [30] J.G. Verwer. Explicit Runge-Kutta methods for parabolic differential equations. *Appl. Num. Math.*, 22:359, 1996.
- [31] R. Verzicco and P. Orlandi. A finite-difference scheme for three-dimensional incompressible flows in cylindrical coordinates. *J. Comp. Phys.*, 123:402, 1996.
- [32] Z. Zheng and L.R. Petzold. Runge-Kutta-Chebyshev projection method. *J. Comp. Phys.*, 219:976, 2006.